Responses to the Comments by Reviewer #2

We are grateful to Reviewer #2 for the helpful suggestions. The manuscript has been revised accordingly. Please note that a new figure is inserted before the original Fig. 5, which now is referred as the Fig. 6. In addition, a new panel of sulfate to SO_2 ratio is added to Fig. 6 as Fig. 6c.

1) *Introduction. GSA is a function of SO2 levels (p 5021 R1, R2, and R3), however, there is little discussion of SO2 sources in the Beijing area. An annual emission of SO2 is given, but not divided into sources. Page 5022 lines 20-30 specifically mention air quality control measures removing automobiles from roadways during the measurement period. However, the relative contribution to the annual SO2 emissions from automobiles and power plants is not given. Are automobiles an important enough source of SO2 to affect GSA production, is the affect on OH from automobile NOx significant, or is primary emission of particles from automobiles the force driving the observations from the air quality control periods, i.e. less surface aerosol surface area leads to higher GSA? The introduction could better set-up the rest of the paper.*

Response: Although GSA productions (shown as R1 to R3) in the atmosphere depend on OH and SO_2, GSA can quickly deposit onto any existing aerosol surfaces. In terms of SO_2 emission sources in Beijing, automobiles are not important. Power plants, domestic heating, and industries respectively account for 49%, 26%, and 24% of the SO_2 emission inventories (Chan and Yao, 2008). The control measures include not only reducing on-road automobile emissions but also temporarily shutting down factory productions around the Beijing area. Although on-road SO_2 was found decreasing during the full control period, a significantly lower aerosol mass loading was also observed, which allowed GSA to accumulate to a higher concentration. We have revised the introduction section to specify the SO_2 emission inventories and to give more details of the air control measures.

2) *p. 5023-5024, Section 2.1 GSA Measurements. The authors claim that GSA is difficult to measure because of its low vapor pressure. However, they also claim to have a custom made, adjustable, GSA primary source. More detail about the calibration source should be given including the uncertainty of the source generation. Twice a week calibrations does not seem frequent enough for a CIMS measurement. Was the whole inlet calibrated? If not, is it known that the inlet wall loss (line 25) was minimized. Were these standard additions onto ambient air with ambient aerosol loadings? What is the sensitivity in Hz per molecule cmˆ-3? How was instrument background determined?*

Response: The calibration device was a 0.5-in OD UV point light source, consisting of a mercury lamp (UVP, 90-0012-01), a bandpass filter centered at 185 ± 25 nm (OMEGA Optical, XB32), and a set of turbulence-inducing fins. During calibration, H_2O molecules in the ambient air were photolyzed by the 184.9 nm radiations into OH radicals, which were converted into GSA (shown as R1-R3) by excess SO_2 (Sigma-Aldrich) supplied in the front of the inlet. The formed GSA concentrations were determined by the H_2O concentration and the 184.9 nm radiation intensity. The H_2O concentration was determined by the ambient temperature and relative humidity obtained from the meteorological station measurements. The 184.9 nm radiation intensity was measured by a CsI phototube (Hamamatsu R5764) certified by the National Institute of Standards and Technology (NIST). Since the 184.9 nm radiation attenuated significantly in the air, a set of fins were used to evenly distribute the

formed GSA inside the inlet. A series of orifices with diameters ranging from 0 to 5 mm were used to vary the light source intensity and the formed GSA concentration.

The uncertainty of the source was determined by the parameters used to calculate the absolute H_2SO_4 standard concentration, which can be measured with good accuracy (uncertainty <2%). The absorption cross section of water at 184.9 nm was taken from literature, with a value of 5.5×10^{-20} cm^2 (JPL, 2006). However, Cantrell et al. (1997) reported a value of 7.14 ($\pm$0.2) $\times 10^{-20}$ cm^2 at 25 °C, with a small positive temperature dependency (4% from 0 to 80 °C). In addition, Parkinson and Yoshino (2003) have obtained a value of 7.0×10^{-20} cm^2 at 22 °C. Hence, the most uncertain parameter was the water absorption cross-section. We estimated the uncertainty associated with the GSA source should be less than 16%, if the average of above literature values was adopted in the calculation. For a 12 s integration time, the instrument sensitivity was about 5×10^4 molecules cm^{-3} per Hz signal.

Since the GSA source was positioned at the front of the inlet, the inlet wall loss should be accounted for by the calibration results. The background signal of the instrument was occasionally checked by covering the drift-tube inlet with a piece of nylon cloth. Due to the high flow rate, only one layer of nylon cloth was used. During daytime background checks, even though the GSA signal decreased substantially, more than ten Hz signal was still observed. However, during nighttime the background check was just a few counts, which was treated as the instrument background.

3) *p. 5025-5026, Section 3.1 Instrument performance and meteorological effect. I am puzzled by the inclusion of this section. I fail to see how it adequately addresses the first sentence, "Accurate measurements of GSA represent a great challenge because of its low concentration". The NSD analysis doesn't address whether or not there are significant inlet losses or if there is inlet effects due to ambient conditions, such as relative humidity. It may be comforting that the signal coming through the inlet exhibits no systematic bias but how is that related to the true ambient conditions. I feeling that showing a time series of GSA signal through calibration, background, and ambient measurement sequence would characterize and define the instrument performance through parameters such as signal to noise ratio and time response. These parameters have better physical meaning than the NSD.*

Response: We have revised the section 3.1 to address the concerns of the reviewer. One of the primary purposes to include section 3.1 was that the instrument was located about 5 m below the attic roof and the inlet can only be positioned toward the east. These physical conditions may cause some bias for the GSA measurements to represent the real ambient level of GSA, especially under curtain wind direction and a high wind speed that can induce turbulence in the front of the inlet, causing wall losses. Since both the calibration device and the instrument performance have been discussed in detail by Zheng et al. (2010), we did not include too much details on the instrument calibrations. As suggested by the reviewer, we have inserted the following two paragraphs to give more detailed descriptions of the calibration device and the instrument performance.

i) "The calibration device was a 0.5-in OD UV point light source, consisting of a mercury lamp (UVP, 90-0012-01), a bandpass filter centered at 185 ± 25 nm (OMEGA Optical, XB32), and a set of turbulence-inducing fins. During calibration, H_2O molecules in the ambient air were photolyzed by the 184.9 nm radiations into OH radicals, which were converted into GSA (shown as R1-R3) by excess SO_2 (Sigma-Aldrich) supplied in the front

of the inlet. The formed GSA concentration was determined by the H_2O concentration and the 184.9 nm radiation intensity. The H_2O concentration was determined by the ambient temperature and relative humidity obtained from the meteorological station measurements. The 184.9 nm radiation intensity was measured by a CsI phototube (Hamamatsu R5764) certified by the National Institute of Standards and Technology (NIST). Since the 184.9 nm radiation attenuated significantly in the air, a set of fins were used to evenly distribute the formed GSA inside the inlet. A series of orifices with diameters ranging from 0 to 5 mm were used to vary the light source intensity and the formed GSA concentration. For a 5 min average time, the detection limit for GSA was about 10^5 molecules cm^{-3}. From in-situ calibrations, the sensitivity of AP-ID-CIMS (counts per second (Hz) per unit H_2SO_4 molecule cm^{-3}) varied within 36% of the mean value (5×10^4 molecules cm^{-3} per Hz signal) and was reported as the uncertainty in the present work. Since the GSA source was positioned at the front of the inlet, the inlet wall loss should be accounted for from the calibration results. The background signal of the API-ID-CIMS was occasionally checked by covering the drift-tube inlet with a piece of nylon cloth. Due to the high flow rate, only one layer of nylon cloth was used. At nighttime when ambient GSA was low, a background signal of a few counts was treated as the instrument background."

ii) "GSA is highly sticky to almost all kind of surfaces. In order to minimize the inlet losses, a short inlet and a high sampling flow rate are used for the GSA measurement, with a similar working principle as a fast-flow reactor (Seeley et al., 1993). The inlet is a 60 cm long 10 cm ID aluminum tube, allowing about 1200 slpm sample flow. The sample residence time is about 0.2 s. Meanwhile, the fast flow rate induces a high Reynolds number turbulent flow with an eddy scale near the diameter of the inlet. Consequently, the small eddies induced by the surface friction are suppressed by the large eddies dominated by the inertial force. GSA sample at the center of the flow must penetrate the small eddies at the edge before colliding with the inlet surface. Hence, inlet losses can be minimized. This is consistent with our ambient test results, showing that the instrument response increases with a higher flow rate with respect to a similar GSA concentration. However, wind gust with a speed of a few m s^{-1} may still impact the inlet flow pattern, especially when the wind direction is perpendicular to the inlet. Figure 2 presents (a) a polar plot of the NSD with wind direction (North = 0 degree) and (b) a scatter plot of NDS with wind direction. Overall, NSD scatters in all wind direction with a slight bias under NW wind, but NSD is symmetrically distributed at any wind speed. This result is explained by the orientation of the inlet, i.e., when wind blows from perpendicular to the inlet or at a higher speed, more wall loss is expected as the air flow changes direction for both cases, but this bias is statistically insignificant."

4) *p. 5027 line 12. Is the mean velocity referring to dry deposition velocity or something else? Please clarify.*

Response: The "*velocity*" is the GSA molecular velocity or the root-mean-square velocity of GSA molecules. The manuscript is revised accordingly.

5) *p. 5027 line 26. Is the 1-sigma error bar the standard deviation of the average or truly the error of the measurement?*

Response: The error bar represents one standard deviation of the average. The manuscript has been revised accordingly.

6) *p. 5027 Equation 3. No NO2 measurement is mentioned in Section 2.2. What NO2 data*

was used in calculating OH? What is the uncertainty in this calculated OH?

Response: NO_2 was routinely measured at the site using a commercial instrument, i.e., Thermo Scientific Model 42C. This information has been inserted into the experimental section. The major uncertainty in the OH calculation originates from the coefficients used in Eq. (3), which is suggested to be valid when NOx is sufficiently high (Ehhalt and Rohrer, 2000). To validate the OH calculation, we use Eq. (3) to estimate the OH concentration at the Yufa site during the Carebeijing2006 field campaign and compare the results with the in-situ measurements. A linear regression between the calculated and the measured OH concentrations shows a slope of 0.89, an intercept of -0.5×10^6 molecules cm^{-3} and a R^2 of 0.6. The negative intercept is caused by the observed nighttime OH, which cannot be reflected by the estimation equation since the observed photolysis frequencies are zero during the night. The correlation and regression results indicate the validity of using above coefficients for Beijing. Given that the Yufa site is located near a highway and influenced by traffic emissions, which is the same as PKU site, we therefore estimate the uncertainty of the OH calculation is around 10% in this work.

7) *p.5028 lines 15-19. I find it hard to follow the one week periodicity in peak GSA values in Figure 3, especially early in the project. I would think there should be meteorological data to support the hypothesis that large-scale weather patterns are causing the periodicity. Expand and briefly discuss the supporting data.*

Response: At the PKU site, the barometric pressure was also found varying sinusoidally with a period of 5 to 10 days. Most of the high GSA episodes were detected during the transitions periods. In addition, higher GSA concentration periods were often associated with northerly wind. Wang et al. (2010) suggested that a week high-pressure system over the Hebei province (to the south of Beijing) led to the two pollution episodes on July 23-29 and August 4-9, when high PM_{10} mass loading (Wang et al., 2010) but low GSA concentration were observed.

8) *p 5029 lines 1-5. The increase in GSA is attributed to the pollution control periods due to a decrease in aerosol surface area, i.e., a decrease in the loss term of equation 2. Did the pollution control measures not affect the production term? What had a larger affect on the loss term, pollution control measures or the periodicity of the large-scale weather patterns? It seems that there could be a few factors influencing GSA levels and there is no attempt to distinguish what is really controlling the GSA.*

Response: Compared to the time period prior to 8 August, more air quality control measures were implemented during the Olympic Games period (8-23 August) to remove more automobiles from the road and to temporary shut down industries around the Beijing area. However, at the PKU site daytime (6 a.m. to 6 p.m.) average SO_2 increased from 3.7 to 4.5 ppbv while aerosol surface area decreased from 1.0×10^3 to 0.57×10^3 μm^2 cm^{-3}. The unexpected increase in SO_2 was probably due to the fact that SO_2 in Beijing was controlled by some regional sources. Meanwhile, the calculated OH concentration increased from 0.4×10^6 to 1.9×10^6 molecules cm^{-3}. Since GSA production can be enhanced by stronger actinic flux and uptake by preexisting aerosol surfaces represents the dominant sink for GSA, an increasing trend in the daily GSA concentration is evident in Fig. 3, especially during the Olympics and Paralympics period, when more stringent air quality control measures were adopted. Consequently, the frequency of the peak H_2SO_4 concentration exceeding 5×10^6 molecule cm^{-3} increases by 16% during August 8-23, compared to the time period prior to August 8. This trend is consistent with that of the frequency of new particle formation events

(Yue et al., 2010).

9) *p. 5029 Section 3.3. I understand that the nucleation events and the MSM analysis are discussed in detail elsewhere. However, without some introduction or summary conclusion details I do not understand what Table 1 is conveying. How are nucleation events defined, especially, in light of conventional instrumentation limitations discussed on p. 5021 line 9? How are GSA and RH related to the calculated formation rate?*

Response: The criterion for discerning these so-called new particle formation events was the burst in the nucleation mode particle concentration (Birmili and Wiedensohler, 2000). In this study, particles between 3 and 10 nm were considered to represent the newly formed particles. One burst was counted as new particle formation event if the duration time was longer than 2.5 h and the maximum number concentration of 3-10 nm particles was larger than 10^4 cm^{-3}. The events with bursts in the 3- to 10-nm size range, lasting a short time but without the growth of 3- to 10-nm particles to larger sizes, were not included in new particle formation events discussed in this study. In the calculation of nucleation rate, the particle number size distributions at ambient RH were used. The particle number size distributions at ambient RH were calculated based on the measured dry number size distributions and the calculated size-dependent hygroscopic growth factors at ambient RH. Hygroscopic growth factors of the nucleation mode particles are obtained from Biskos et al. (2009), and those of larger particles are calculated from our earlier measurements size dependently at 90% RH (Laakso et al., 2004).

10) *p. 5029 – 5030 Section 3.4 and Figure 5. The sulfate production from is very small, peaking at 0.014 and 0.05 ug m-3 hr-1 for Aitken and accumulation modes, respectively. It would take over a day at the peak sulfate production from GSA rate to account for the observed sulfate increases. This seems too slow to be a significant contributor to the total sulfate mass. The increases in measured sulfate seem to be visually enhanced by the range of the axis chosen. For example. In 5a, the production rate increases by a factor of 6 from 0800 to the peak at 1300, while the measured sulfate only increases by ~20% in the same time period. Obviously, there is much more sulfate measured than can be accounted for by GSA production. Where is that coming from? The manuscript should be strengthened by discussing the contribution of GSA to the sulfate budget. I also wonder if analyzing hourly average diurnal profiles over ~ 80 days is the best way to look at the data. The observations span multiple emission control periods and large-scale weather events. Has the effect of sulfate production from GSA been averaged out over the different periods? Fig. 3 shows that absolute GSA levels differ during the different periods. Does sulfate production differ, too?*

Response: The scales of Fig. 6a and 6b have been revised accordingly. The typical GSA to aerosol sulfate conversion process can be demonstrated by Fig. 5, which displays the GSA time series from 23 to 25 August, i.e., a nucleation day followed by two relatively polluted days. The calculated GSA trace appears to match the observation very well except on 23 August, since nucleation is not accounted for in Eq. (2). The simulated high GSA concentration on August 23 is the result of low aerosol surface area, since all air pollutants appears to be low at the same time. Therefore, we believe that GSA is primarily generated from OH + SO_2 reactions and transferred into the aerosol phase through either nucleation or condensation onto existing aerosol surfaces.

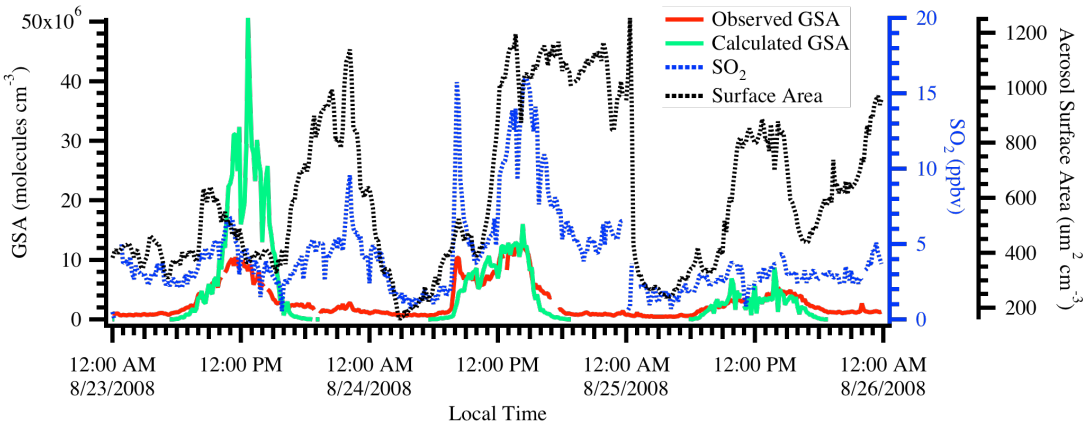

Figure 5. Time series of both observed (red trace) and calculated (green trace) GSA from 23 to 25 August. Also shown here are the SO_2 (blue dot) and aerosol surface area (black dot) used in GSA simulations.

Since SO_2 in Beijing is controlled by regional sources and aerosol sulfate can be suspended in the air for several days, the sulfate measured at the PKU site has an oxidation history that cannot be explained by local GSA measurements. The high sulfate concentration measured at the PKU site may be a result of accumulated oxidation process, occurring over many days since the time of SO_2 emission. Moreover, the GSA productions are likely much higher in the source regions, which are primarily industrial areas with much more concentrated SO_2. As shown in Fig. 6c, the PM_1 sulfate to SO_2 ratio significantly reduces the diurnal variation of sulfate, indicating that most aerosol sulfate has been formed before arriving at the PKU site. Therefore, it is reasonable to use the hour-average of the whole data set to investigate the correlation between the aerosol sulfate and GSA. Assuming the same GSA production rate from the source region to the PKU site, we obtain an average of 0.6 μg m^{-3} per day sulfate production from the GSA condensation. Given that $PM_{1.0}$ sulfate has a daily average concentration of ~17 μg m^{-3} and a residence time of 3 to 7 days, GSA condensation can contribute to 10 – 25% of PM_1 sulfate. Moreover, the slight decreasing trend in Fig. 6c indicates that air mass with less sulfate but more SO_2 is mixed down, which makes sulfate productions through cloud processing less likely.

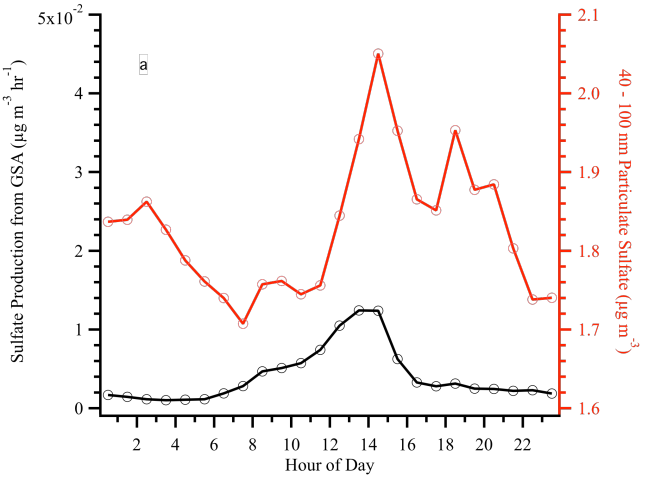

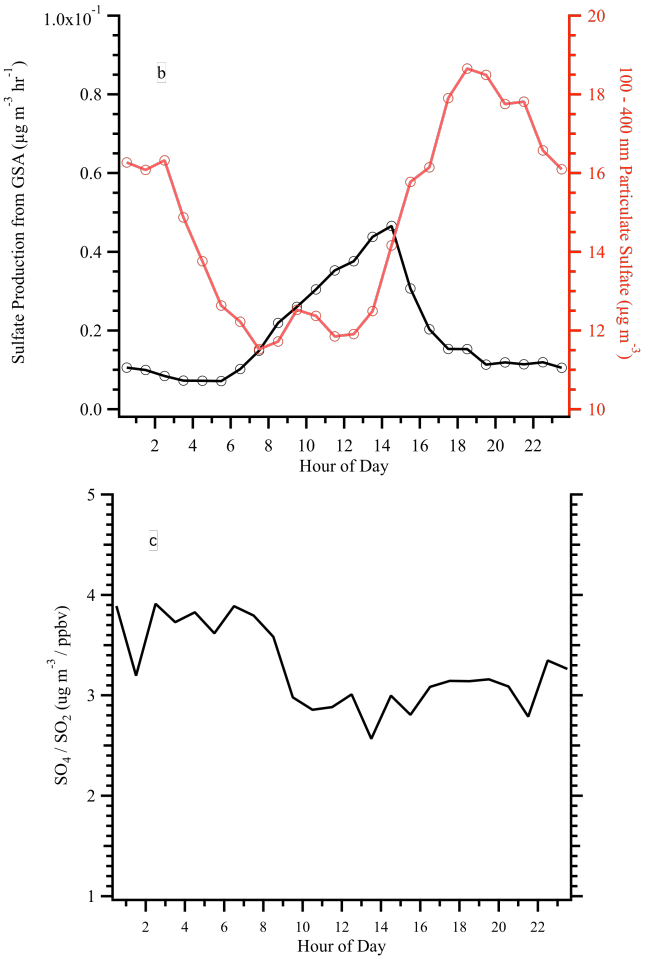

Figure 6. (a) Diurnal profiles of condensation rates of GSA onto Aitken mode aerosols (40-100 nm) and sulfate concentrations in Aitken mode; (b) Diurnal profiles of condensation rates of GSA onto accumulation mode particles (100-400 nm) and sulfate concentrations in accumulation mode; (c) Diurnal profile of PM_1 sulfate (SO_4) to SO_2 ratio.

11) p. 5030 lines 21-23. This sentence is confusing. Since biomass burning and automobile exhaust contribute to fine particles why does it follow that secondary sources can, too?

Response: We have revised the sentence as "It has been suggested by Guo et al. (2010) that fine mode sulfate in the Beijing area can mainly arise from secondary sources, since no indications of primary contributions from either biomass burning or automobile exhausts were found."

12) p. 5040 Figure 3. The arrows do a poor job of separating the different control measure regimes. I suggest light background shading for the different time periods.

Response: We have replaced the arrows with dashed lines in Fig. 3 to divide different control periods.

13) p. 5041 Figure 4. What are the estimated uncertainties in the OH calculation and the simulated GSA curves?

Response: The major uncertainty in the OH calculation originate from the coefficients used in Eq. (3), which is suggested to be valid when NOx is sufficiently high (Ehhalt and Rohrer, 2000). To validate the OH calculation, we use Eq. (3) to estimate the OH concentration at the Yufa site during the Carebeijing2006 field campaign and compare the results with the in-situ measurements. A linear regression between the calculated and the measured OH concentrations shows a slope of 0.89, an intercept of -0.5×10^6 molecules cm^{-3} and a R^2 of 0.6. The negative intercept is caused by the observed nighttime OH, which cannot be reflected by the estimation equation since the observed photolysis frequencies are zero during the night. The correlation and regression results indicate the validity of using above coefficients for Beijing. Given that the Yufa site is located near a highway and influenced by traffic emissions, which is the same as PKU site, we therefore estimate the uncertainty of the OH calculation is around 10% in this work. Each variable used to simulate GSA (except OH) can be measured with a reasonable accuracy (much less than 1%). Therefore, we believe OH is responsible for most of the uncertainty of the GSA simulation, which is about 10%.

14) p. 5042 Figure 5. The traces in Fig. 5 are lighter than in Fig. 4 and the symbols are open not filled in making it harder to read.

Response: We have modified the Fig. 6, using thicker traces and bigger symbols.

References:

Birmili, W., and Wiedensohler, A.: New particle formation in the continental boundary layer: Meteorological and gas phase parameter influence, Geophys. Res. Letts., 27, 3325-3328, 2000.

Biskos, G., Buseck, P. R., and Martin, S. T.: Hygroscopic growth of nucleation-mode acidic sulfate particles, J. Aerosol Sci, 40, 338-347, doi:10.1016/j.jaerosci.2008.12.003, 2009.

Cantrell, C. A., Zimmer, A., and Tyndall, G. S.: Absorption cross sections for water vapor from 183 to 193 nm, Geophys. Res. Letts., 24, 2195-2198, 1997.

Chan, C. K., and Yao, X.: Air pollution in mega cities in China, Atmos. Environ., 42, 1-42, doi:10.1016/j.atmosenv.2007.09.003, 2008.

Ehhalt, D. H., and Rohrer, F.: Dependence of the OH concentration on solar UV, J. Geophys. Res., 105, 3565-3571, 2000.

JPL: Chemical kinetics and photochemical data for use in atmospheric studies Evaluation 15, NASA, JPL, Caltech, Pasadena, Calif., 523 p. pp., 2006.

Laakso, L., Petaja, T., Lehtinen, K. E. J., Kulmala, M., Paatero, J., Horrak, U., Tammet, H., and Joutsensaari, J.: Ion production rate in a boreal forest based on ion, particle and radiation measurements, Atmos. Chem. Phys., 4, 1933-1943, 2004.

Parkinson, W. H., and Yoshino, K.: Absorption cross-section measurements of water vapor in the wavelength region 181-199 nm, Chem. Phys., 294, 31-35, 10.1016/s0301-0104(03)00361-6, 2003.

Wang, T., Nie, W., Gao, J., Xue, L. K., Gao, X. M., Wang, X. F., Qiu, J., Poon, C. N., Meinardi, S., Blake, D., Wang, S. L., Ding, A. J., Chai, F. H., Zhang, Q. Z., and Wang, W. X.: Air quality during the 2008 Beijing Olympics: secondary pollutants and regional impact, Atmos. Chem. Phys., 10, 7603-7615, doi:10.5194/acp-10-7603-2010, 2010.

Zheng, J., Khalizov, A., Wang, L., and Zhang, R.: Atmospheric Pressure-Ion Drift Chemical Ionization Mass Spectrometry for Detection of Trace Gas Species, Anal. Chem., 82, 7302-7308, doi:10.1021/ac101253n, 2010.